
DKL-KAN: SCALABLE DEEP KERNEL LEARNING USING KOLMOGOROV-ARNOLD NETWORKS

A PREPRINT

✉ **Shrenik Zinage***

School of Mechanical Engineering
Purdue University
West Lafayette, IN
szinage@purdue.edu

✉ **Sudepta Mondal**

RTX Technology Research Center,
411 Silver Lane,
East Hartford, CT
sudepta.mondal2@rtx.com

✉ **Soumalya Sarkar**

RTX Technology Research Center,
411 Silver Lane,
East Hartford, CT
soumalya.sarkar@rtx.com

August 1, 2024

ABSTRACT

The need for scalable and expressive models in machine learning is paramount, particularly in applications requiring both structural depth and flexibility. Traditional deep learning methods, such as multilayer perceptrons (MLP), offer depth but lack ability to integrate structural characteristics of deep learning architectures with non-parametric flexibility of kernel methods. To address this, deep kernel learning (DKL) was introduced, where inputs to a base kernel are transformed using a deep learning architecture. These kernels can replace standard kernels, allowing both expressive power and scalability. The advent of Kolmogorov-Arnold Networks (KAN) has generated considerable attention and discussion among researchers in scientific domain. In this paper, we introduce a scalable deep kernel using KAN (DKL-KAN) as an effective alternative to DKL using MLP (DKL-MLP). Our approach involves simultaneously optimizing these kernel attributes using marginal likelihood within a Gaussian process framework. We analyze two variants of DKL-KAN for a fair comparison with DKL-MLP: one with same number of neurons and layers as DKL-MLP, and another with approximately same number of trainable parameters. To handle large datasets, we use kernel interpolation for scalable structured Gaussian processes (KISS-GP) for low-dimensional inputs and KISS-GP with product kernels for high-dimensional inputs. The efficacy of DKL-KAN is evaluated in terms of computational training time and test prediction accuracy across a wide range of applications. Additionally, the effectiveness of DKL-KAN is also examined in modeling discontinuities and accurately estimating prediction uncertainty. The results indicate that DKL-KAN outperforms DKL-MLP on datasets with a low number of observations. Conversely, DKL-MLP exhibits better scalability and higher test prediction accuracy on datasets with large number of observations.

Keywords Gaussian Process Regression · Deep Kernel · Kolmogorov-Arnold Network · Multilayer Perceptron

1 Introduction

During the 1990s, before the emergence of deep learning, Gaussian Processes (GP) (Williams and Rasmussen [2006]) became popular as alternatives to neural networks (NN) because of their ability to quantify uncertainty and their often superior performance. During this period, benchmarking datasets primarily consisted of tabular data, leading to the perception that representation learning could be entirely bypassed, focusing solely on the relationship between vectors in the input space. However, in the early 2010s, the community’s focus shifted towards more intricate domains such as sequences (Mikolov et al. [2010]), images (Krizhevsky et al. [2012]), and speech (Hinton et al. [2012]), driven by a series of works leveraging the inductive biases of domain-specific NNs. This shift posed a challenge for GPs, primarily due to the difficulty in tailoring kernels that express useful inductive biases for these diverse domains. In response to these challenges, researchers proposed methods for learning GP kernels directly from data (Wilson and Adams [2013]), aiming to improve the adaptability of GPs to diverse datasets by automatically capturing relevant features.

GP (Williams and Rasmussen [2006]) are favored in Bayesian modeling due to their transparent interpretability and reliable uncertainty quantification. Typically, these models involve a few kernel hyperparameters optimized with respect to the marginal likelihood. Nonetheless, for many common choices, the kernel remains fixed, restricting the capability of GP to learn representations from the data that could improve predictions, thereby functioning primarily as smoothing mechanisms. This restricts the applicability of GP to data that is high-dimensional and highly structured. Conversely, deep neural networks (DNN) (LeCun et al. [2015]) are renowned for learning strong representations which are utilized for predicting unseen test inputs. Despite their good performance, deterministic NN tend to produce overconfident predictions (Guo et al. [2017]) and lack trustworthy uncertainty estimates. The Bayesian approach to NN aims to mitigate these challenges; however, despite recent progress in variational inference and sampling techniques, inference in Bayesian NN remains difficult due to complicated posteriors and the huge number of parameters. Additionally, Bayesian NNs generally require multiple forward passes to obtain several samples of the predictive posterior to average over. Consequently, it is logical to combine the uncertainty representation advantages of GPs with the representation-learning advantages of NNs to leverage the strengths of both. This gave rise to deep kernel learning (DKL) (Wilson et al. [2016a]) which uses an NN to extract meaningful representations that are subsequently fed into a standard GP, allowing for end-to-end learning of all model parameters. Both kernel hyperparameters and network parameters can be jointly trained by using variational inference or maximizing the marginal likelihood. In Wilson et al. [2016a], DKL has shown to outperform conventional shallow kernel learning methods, such as the radial basis function (RBF) kernel and standard NNs on a wide range of applications.

Multilayer perceptrons (MLP) (Haykin [1998]), a cornerstone of modern deep learning, consist of multiple layers of nodes, including an input layer, one or more hidden layers, and an output layer. These networks are capable of learning complex non-linear relationships within data, as evidenced by the universal approximation theorem (Hornik et al. [1989]). Despite their success, MLP are often criticized for their lack of interpretability Cranmer [2023], susceptibility to overfitting, scalability, and issues related to vanishing or exploding gradients during training.

Kolmogorov-Arnold Networks (KAN) (Liu et al. [2024]) have garnered significant attention lately as a novel neural network architecture aimed at addressing some of the inherent limitations of MLP. The foundation of KAN lies in the Kolmogorov-Arnold representation theorem, which asserts that any multivariate continuous function can be expressed as a finite sum of univariate functions and addition operations. This theorem, initially proven by Kolmogorov in 1957 to solve Hilbert’s 13th problem (Kolmogorov [1957], Braun and Griebel [2009]), laid the groundwork for various neural network designs that leverage its decomposition principles. Unlike MLP, which rely on linear weights and fixed activation functions, KAN use learnable activation functions, typically implemented as splines or B-splines. This design choice allows KANs to adaptively shape their activation functions to better fit the underlying data, thereby improving both accuracy and interpretability.

The main contributions of this paper are as follows. First, we introduce a scalable deep kernel using KAN (DKL-KAN) as an alternative to the traditional DKL using MLP (DKL-MLP). Additionally, we present a comparative analysis of two DKL-KAN configurations: one matching the neuron and layer count of DKL-MLP, and another with a similar number of trainable parameters, ensuring a rigorous evaluation against the baseline. Our method is tested across various benchmark UCI regression datasets (Evans [2021]), focusing on both computational training time and prediction accuracy. Additionally, we also investigate the efficacy of DKL-KAN in modeling discontinuities and accurately calculating uncertainty bounds. To address the challenges of large datasets, we use Kernel Interpolation for Scalable Structured Gaussian Processes (KISS-GP) (Wilson and Nickisch [2015]) for low input dimensions and KISS-GP with scalable kernel interpolation for product kernels (SKIP) (Gardner et al. [2018]) for high-dimensional inputs. The remainder of the paper is organized as follows. Section 2 discusses the related works. Section 3 delves into the brief explanation of KAN. This is followed by explanation of GP in Section 4. The findings of this study are detailed in Section 5, and finally, the conclusions are succinctly presented in Section 6

2 Related Works

2.1 Gaussian Process

GPs, traditional nonparametric modeling tools and NNs, known for their flexibility in fitting complex data patterns, have an intriguing equivalence (Neal and Neal [1996], Lee et al. [2017], Matthews et al. [2018], Garriga-Alonso et al. [2018], Novak et al. [2018], Yang [2019]). As derived by Neal and Neal [1996], in the limit of infinite width, a one-layer NN corresponds to a GP. This equivalence implies that for infinitely wide networks, an i.i.d. prior over weights and biases can be replaced with a corresponding GP prior over functions, allowing exact Bayesian inference for regression using NNs.

The concept of DKL was first presented by Wilson et al. [2016a], building upon the framework of KISS-GP (Wilson and Nickisch [2015]). This approach combines deep NN with traditional covariance functions using local kernel

interpolation to create complicated kernels. Although DKL excels in approximating intricate kernels for GP, it exhibits notable drawbacks. It does not support stochastic gradient training and is inadequate for classification tasks. In this regard, Wilson et al. [2016b] introduced the stochastic variational deep kernel learning approach, which allows the model in performing classification tasks, multi-task learning, and stochastic gradient optimization. Calandra et al. [2016] extended the general framework by introducing manifold GP, which involve applying a kernel function to a parameterized transformation of the input data. This transformation can be parameterized using NN. The study of intricate kernel learning has also been a focus within certain specialized fields. For instance, Al-Shedivat et al. [2017] used a recurrent neural network to acquire kernels characterized by recurrent patterns. In contrast, Achituve et al. [2021] explored using NN to learn a shared kernel function within the context of personalized federated learning. There has also been initiatives aimed at the regularization of models based on DKL. Liu et al. [2021] introduced a latent-variable framework that integrates a stochastic encoding of inputs to allow regularized representation learning. Recently, Achituve et al. [2023] introduced an innovative methodology for training DKL. This method uses the uncertainty quantification from a GP with an infinite-width deep NN kernel to steer the optimization of DKL.

The flexibility of deep NN can however lead to overfitting in DKL models, as identified by Ober et al. [2021]. They discovered that DKL often correlates all input data points in an effort to minimize the effect of the complexity penalty term in the marginal likelihood. This challenge was tackled by using full Bayesian inference over the network parameters using Markov Chain Monte Carlo (MCMC) techniques. However, MCMC is inefficient when dealing with high-dimensional posteriors. To address this, Matias et al. has introduced amortized variational DKL, which leverages deep NN to generate embeddings for the kernel function and to learn variational distributions over inducing points, thereby reducing overfitting by locally smoothing predictions.

2.2 Kolmogorov-Arnold Networks

Recent research has proposed several extensions and variants of KANs to improve their performance and reduce computational complexity. For instance, Fourier KAN (Xu et al. [2024]), Wavelet KAN (Bozorgasl and Chen [2024]), RBF-KAN (Li [2024]), fractional KAN (Aghaei [2024a]), BSRBF-KAN (Ta [2024]), rKAN (Aghaei [2024b]) and sineKAN (Reinhardt and Gleyzer [2024]) replace B-splines with other function bases to achieve more accurate solutions. Another notable variant is the Chebyshev KAN (SS [2024]), which use orthogonal polynomials as univariate functions. Each of these variants aims to address specific limitations or improve certain capabilities of the original KAN architecture. KANs have also shown promise in the context of solving partial differential equations and operator learning (Liu et al. [2024], Shukla et al. [2024]). Reference Wang et al. [2024] combined KANs with physics-informed neural networks (PINNs) to address the 2D Poisson equation, achieving superior performance compared to traditional methods. Similarly, Abueidda et al. [2024] introduced DeepOKAN, an RBF-based KAN operator network, for solving 2D orthotropic elasticity problems. These studies highlighted the potential of KANs to tackle complex scientific computing tasks more effectively than MLPs. The efficacy of KANs has also been explored in various other applications, including computer vision (Azam and Akhtar [2024]), medical image segmentation (Li et al. [2024]), and learning graphs (Kiamari et al. [2024]). However, despite these advancements, the scalability and computational efficiency of KANs remain significant challenges (Liu et al. [2024]).

3 Kolmogorov-Arnold Networks

KANs represent an innovative class of neural networks that leverage the theoretical insights provided by the Kolmogorov-Arnold representation theorem. This theorem provides a theoretical basis for expressing any multivariate continuous function as a finite composition of univariate continuous functions and additions. By exploiting this theorem, KANs aim to overcome some of the limitations associated with traditional neural network architectures, particularly in terms of function approximation and interpretability. This theorem, also known as the superposition theorem, is a fundamental result in approximation theory. It asserts that any continuous multivariate function on a bounded domain can be represented as a composition of a finite number of univariate functions and linear operations. Assuming a smooth known function $f : [0, 1]^k \rightarrow \mathbb{R}$, continuous univariate functions $\phi_{i,j} : [0, 1] \rightarrow \mathbb{R}$, and continuous functions $\psi_j : \mathbb{R} \rightarrow \mathbb{R}$, the theorem states:

$$f(\mathbf{x}) = \sum_{j=1}^{2k+1} \psi_j \left(\sum_{i=1}^k \phi_{i,j}(x_i) \right), \quad (1)$$

for some k . Irrespective of the chosen functions, an L layer deep KAN can be expressed in matrix form as follows:

$$\hat{f}(x) = (\Psi_{L-1} \circ \dots \circ \Psi_1 \circ \Psi_0)(x),$$

where each Ψ_l represents the function matrix of the l^{th} KAN layer. If n_l denotes the number of neurons in layer l , then the functional matrix Ψ_l that links neurons in layer l to those in layer $l + 1$ is defined as follows:

$$\Psi_l = \begin{pmatrix} \phi_{1,1}(\cdot) & \phi_{1,2}(\cdot) & \cdots & \phi_{1,n_l}(\cdot) \\ \phi_{2,1}(\cdot) & \phi_{2,2}(\cdot) & \cdots & \phi_{2,n_l}(\cdot) \\ \vdots & \vdots & \vdots & \vdots \\ \phi_{n_{l+1},1}(\cdot) & \phi_{n_{l+1},2}(\cdot) & \cdots & \phi_{n_{l+1},n_l}(\cdot) \end{pmatrix},$$

where $\phi_{i,j}$ signifies the activation function connecting neuron i in layer l to neuron j in layer $l + 1$. Let \mathcal{D} denote the derivative operator and ϵ be a constant based on the behaviour of $f(\cdot)$. The convergence of this approximation is characterized by:

$$\max_{|\gamma| \leq m} \sup_{x \in [0,1]^k} \left\| \mathcal{D}^\gamma \left\{ \hat{f}(x) - f(x) \right\} \right\| < \epsilon.$$

For more details, please refer to Liu et al. [2024].

The first KAN paper (Liu et al. [2024]) introduced the residual activation function $\phi(x)$, which is defined as the sum of the base function $b(x) = \text{silu}(x)$ and the spline function $s(x)$, each multiplied by their respective weight matrices w_b and w_s . This spline function $s(x)$ is represented as a linear combination of B-splines $B_i(x)$:

$$s(x) = \sum_i c_i B_i(x),$$

where c_i are trainable constants. The activation function is configured with $w_s = 1$ and $s(x) \approx 0$, and w_b is initialized using Xavier initialization. The residual activation function is then given by:

$$\phi(x) = w_b b(x) + w_s s(x).$$

Due to the high computational cost of KANs, a more efficient variant was introduced in Blealtan [2024]. This version follows the methodology of Liu et al. [2024] but optimizes the computations using B-spline basis functions combined linearly, thereby reducing memory usage and simplifying the computational process. The authors also replaced the incompatible L1 regularization on input samples with L1 regularization on weights, incorporated learnable scales for activation functions, and changed the initialization of the base weight and spline scaler matrices to Kaiming uniform initialization. These modifications significantly improved performance on the MNIST dataset. In this paper, we utilize this efficient KAN for comparison with MLP.

4 Gaussian Processes

GP is a probabilistic non-parametric approach which defines a prior over functions and can be utilized for regression tasks. A GP is exhaustively described by its mean function, $m(\mathbf{x})$, and a covariance function known as the kernel function, $k(\mathbf{x}, \mathbf{x}')$. Importantly, for any finite set of inputs, a GP will output a multivariate Gaussian distribution. In the context of GPR, the underlying assumption is that the function to be approximated is a sample from a GP. The mean function, $m(\mathbf{x})$, and covariance function, $k(\mathbf{x}, \mathbf{x}')$, are represented by the equations:

$$\begin{aligned} m(\mathbf{x}) &= \mathbb{E}[f(\mathbf{x})], \\ k(\mathbf{x}, \mathbf{x}') &= \mathbb{E}[(f(\mathbf{x}) - m(\mathbf{x}))(f(\mathbf{x}') - m(\mathbf{x}'))]. \end{aligned}$$

In practice, it is common to use a constant mean function, i.e., $m(\mathbf{x}) = c$, and focus on defining the covariance function. The covariance function, measures the similarity between data points. One common choice is the standard radial basis function (RBF) kernel. Assuming σ^2 as the signal variance, l_d representing the length scales for each dimension, and D indicating the number of dimensions, we have:

$$k(\mathbf{x}, \mathbf{x}') = \sigma^2 \exp \left(- \sum_{d=1}^D \frac{(x_d - x'_d)^2}{2l_d^2} \right).$$

The length scales l_d control the relevance of different dimensions. When l_d is small, changes in the d -th dimension have a large effect on the covariance, making that dimension more relevant.

Given a dataset \mathcal{D} of n input vectors, $X = \{\mathbf{x}_1, \dots, \mathbf{x}_n\}$, each having dimension D , these index an $n \times 1$ vector of targets $\mathbf{y} = (y(\mathbf{x}_1), \dots, y(\mathbf{x}_n))^T$. Assuming the presence of additive Gaussian noise, the relationship between the target $y(\mathbf{x})$ and a function $f(\mathbf{x})$ can be modeled as:

$$y(\mathbf{x}) \mid f(\mathbf{x}) \sim \mathcal{N}(y(\mathbf{x}); f(\mathbf{x}), \sigma_y^2),$$

where σ_y^2 is the variance of the noise. Assuming all covariance matrices implicitly rely on the kernel hyperparameters θ , we have the predictive distribution of the GP at the n_* test points indexed by X_* to be expressed as:

$$\begin{aligned} \mathbf{f}_* | X_*, X, \mathbf{y}, \boldsymbol{\theta}, \sigma_y^2 &\sim \mathcal{N}(\mathbb{E}[\mathbf{f}_*], \text{cov}(\mathbf{f}_*)), \\ \mathbb{E}[\mathbf{f}_*] &= m(X_*) + k_\theta(X_*, X) [k_\theta(X, X) + \sigma_y^2 I]^{-1} \mathbf{y} \\ \text{cov}(\mathbf{f}_*) &= k_\theta(X_*, X_*) - k_\theta(X_*, X) [k_\theta(X, X) + \sigma_y^2 I]^{-1} k_\theta(X, X_*), \end{aligned}$$

where,

$$\mathbf{f}_* = f_*(X) = [f_*(\mathbf{x}_1), \dots, f_*(\mathbf{x}_{n_*})]^\top.$$

Here, $k_\theta(X_*, X)$ is an $n_* \times n$ matrix of covariances between the GP evaluated at X_* and X . Additionally, $m(X_*)$ designates the $n_* \times 1$ mean vector, and $k_\theta(X, X)$ represents the $n \times n$ covariance matrix evaluated at training inputs X . The conditional probability density of the target variable \mathbf{y} , given the parameters θ and input data X , can be expressed as:

$$\log p(\mathbf{y} | \theta, X) \propto - \left[\mathbf{y}^\top (k_\theta(X, X) + \sigma^2 I)^{-1} \mathbf{y} + \log |k_\theta(X, X) + \sigma^2 I| \right].$$

4.1 Deep kernel

A deep kernel integrates a neural network with a traditional kernel function, improving the model’s ability to capture complex patterns in data. The neural network effectively compresses and distills the input space, mapping it to a lower-dimensional representation that is more informative for the GP model. The transformation induced by the neural network can allow the model to fit more complicated, non-smooth, and anisotropic functions, unlike the standard kernels like RBF, which model smooth and isotropic functions. Also, by mapping a high-dimensional input space to a lower-dimensional one using a neural network, we can mitigate the curse of dimensionality. This makes the GPR more tractable and can improve its generalization by focusing on the most informative dimensions of the data.

Assuming $\phi(\mathbf{x}; \beta)$ is a nonlinear mapping given by a neural network parameterized by β , and $k(\mathbf{x}_i, \mathbf{x}'_j | \alpha)$ representing the standard RBF kernel parameterized by α , we transform the inputs as:

$$k(\mathbf{x}_i, \mathbf{x}'_j | \alpha) \rightarrow k(\phi(\mathbf{x}_i; \beta), \phi(\mathbf{x}'_j; \beta) | \alpha, \beta).$$

We investigate the effectiveness of using KANs for DKL in this study. Fig. 1 shows the schematic of DKL-KAN with three inputs and one output. We simultaneously optimize all deep kernel hyperparameters, denoted as $\gamma = (\alpha, \beta)$, by maximizing the log marginal likelihood \mathcal{L} of the exact GP. To compute the derivatives of \mathcal{L} with respect to γ , we use the following chain rule:

$$\frac{\partial \mathcal{L}}{\partial \alpha} = \frac{\partial \mathcal{L}}{\partial k_\gamma(X, X)} \frac{\partial k_\gamma(X, X)}{\partial \alpha}, \quad \frac{\partial \mathcal{L}}{\partial \beta} = \frac{\partial \mathcal{L}}{\partial k_\gamma(X, X)} \frac{\partial k_\gamma(X, X)}{\partial \phi(\mathbf{x}_i; \beta)} \frac{\partial \phi(\mathbf{x}_i; \beta)}{\partial \beta}.$$

The implicit derivative of the log marginal likelihood with respect to covariance matrix $k_\gamma(X, X)$ is expressed as

$$\frac{\partial \mathcal{L}}{\partial k_\gamma(X, X)} = \frac{1}{2} (k_\gamma(X, X)^{-1} \mathbf{y} \mathbf{y}^\top k_\gamma(X, X)^{-1} - k_\gamma(X, X)^{-1}),$$

where the noise covariance $\sigma^2 I$ is included within the covariance matrix and is considered part of the base kernel hyperparameters α .

A significant computational challenge in DKL is resolving the linear system $(k_\gamma(X, X) + \sigma^2 I)^{-1} \mathbf{y}$. Additionally, within the realm of kernel learning, evaluating the logarithm of the determinant $\log |k_\gamma(X, X) + \sigma^2 I|$ as part of the marginal likelihood presents another difficulty. The conventional method uses the Cholesky decomposition of the $n \times n$ matrix $k_\gamma(X, X)$, which requires $\mathcal{O}(n^3)$ operations and $\mathcal{O}(n^2)$ storage. After completing inference, the computation of the predictive mean entails a cost of $\mathcal{O}(n)$, while calculating the predictive variance incurs a cost of $\mathcal{O}(n^2)$ for each test point \mathbf{x}_* .

4.2 Scaling to large datasets for low input dimensions

Due to the cubic scaling of computations with the number of data points in the previously mentioned approach, we use structural kernel interpolation (SKI) using local cubic kernel interpolation to construct GP models for large datasets (Wilson and Nickisch [2015], Wilson et al. [2015]). Many strategies to scale GP models for large datasets belong to the class of inducing point methods (Snelson and Ghahramani [2005], Hensman et al. [2013], Silverman [1985]).

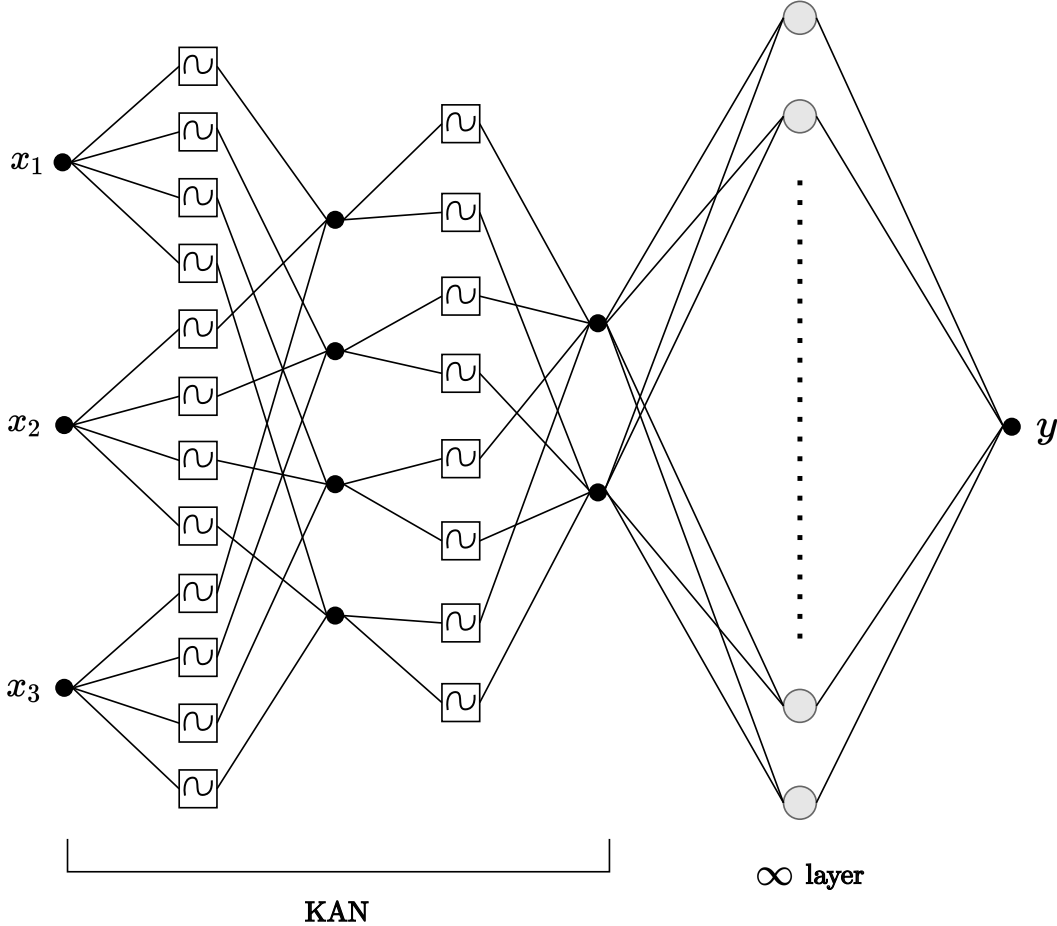


Figure 1: Schematic of DKL-KAN with 3 inputs and 1 output

These methods replace the exact kernel with an approximation to accelerate computations. For m inducing points, the approximate kernels lead to computational complexity of $\mathcal{O}(m^2n + m^3)$ and storage complexity of $\mathcal{O}(mn + m^2)$ for GP inference and learning (Quinero-Candela and Rasmussen [2005]), resulting in a predictive mean and variance cost of $\mathcal{O}(m)$ and $\mathcal{O}(m^2)$ per test case. Nevertheless, when using a limited number of inducing points, these techniques experience a considerable decline in accuracy (Wilson [2014]). In contrast, methods that exploit structural properties, like Kronecker (Saatçi [2012]) and Toeplitz (Cunningham et al. [2008]), leverage the covariance matrix to achieve scalable inference and learning without relying on approximations, thereby preserving both scalability and predictive precision. However, the necessity of an input grid limits the applicability of these methods to most problems. SKI (Wilson and Nickisch [2015]) integrates the benefits of both inducing point and structure-exploiting methods, explaining how the accuracy and efficiency of an inducing point method depend on the number of inducing points, kernel choice, and interpolation method. By selecting different interpolation strategies for SKI, novel inducing point methods can be devised. KISS-GP (Wilson and Nickisch [2015]) uses SKI with local cubic and inverse distance weight interpolation to create a sparse approximation to the cross-covariance matrix between inducing points and original training points. Hence to ensure scalability, we replace all occurrences of $k_\gamma(X, X)$ with the KISS-GP covariance matrix

$$k_\gamma(X, X) \approx Wk_\gamma(U, U)W^\top,$$

where W represents a sparse matrix of interpolation weights, containing only four non-zero elements per row for local cubic interpolation. The term $k_\gamma(U, U)$ is a covariance matrix derived from the deep kernel, evaluated over m latent inducing points $U = [\mathbf{u}_i]_{i=1\dots m}$. The computational complexity for KISS-GP training is $\mathcal{O}(n + h(m))$, with $h(m)$ being nearly linear in m . The ability to have $m \approx n$ enables KISS-GP to achieve near-exact accuracy in its approximation, maintaining a non-parametric representation while ensuring linear scaling in n and $\mathcal{O}(1)$ time per test

point prediction. This approach is especially efficient when the input dimensionality is less (generally less than four), as the cost of grid construction escalates exponentially with the amount of data.

4.3 Scaling to large datasets for high input dimensions

To tackle the aforementioned problem, we use SKIP as introduced by Gardner et al. [2018]. SKIP is designed to handle large datasets with high-dimensional inputs efficiently. It comprises of two primary elements: SKI and the product kernel structure. The product kernel structure in SKIP mitigates the curse of dimensionality inherent in SKI. For data characterized by d input dimensions and denoting \otimes as element-wise multiplication, the kernel matrix within the product kernel structure is represented as:

$$k_\gamma(X, X) = k_\gamma(X, X)^{(1)} \otimes \dots \otimes k_\gamma(X, X)^{(d)}.$$

This formulation ensures that SKIP maintains linear time complexity, even when dealing with high dimensional inputs.

5 Experiments

5.1 Data normalization

All the training datasets were normalized using empirical cumulative distribution function technique prior to the initiation of the training process. This normalization technique transforms data into a uniform distribution, which can be particularly useful if the original distribution is unknown or if the data does not follow a Gaussian distribution which is a common assumption in many machine learning algorithms. It is also more robust to outliers as it ranks the datapoints rather than directly scaling their values.

5.2 Results

The GP models and deep kernel is programmed using GPyTorch library respectively with a PyTorch backend. We set the loss function as negative of exact marginal log likelihood and the optimizer used is Adam with tuned hyperparameters. We set the learning rate as 0.075 with an exponential decay rate of 0.997 for smooth convergence of the loss. The GP models are trained for a total of 2500 epochs with a patience of 1000 epochs. All training is performed on an NVIDIA A100-SXM4-40GB GPU (1 GPU with 512 GB RAM). The codes for this paper will be made available at <https://github.com/shrenikvz/dkl-kan> upon publication.

5.2.1 UCI regression datasets

We evaluate our models on a diverse set of benchmark UCI regression problems with varying sizes and characteristics. The base kernel is fixed as the RBF kernel. For DKL approaches, we reduce the dimensionality to 2 before feeding it to the base kernel. The neural network architecture for DKL-MLP consists of three hidden layers with 1000, 500, and 50 neurons, respectively. To fairly compare DKL-KAN with DKL-MLP, we train two models using KANs: DKL-KAN1 and DKL-KAN2. DKL-KAN1 has the same number of neurons and layers as DKL-MLP, while DKL-KAN2 has approximately the same number of trainable parameters as DKL-MLP. DKL-KAN2’s architecture includes three hidden layers with 256, 128, and 64 neurons, respectively. We utilize RMSE as the metric to evaluate the test prediction accuracy.

Given that GP models could be trained in a finite time for datasets with fewer than 20,000 observations, we use SKI exclusively for datasets exceeding 20,000 observations. For these larger datasets, we use KISS-GP for DKL-MLP, DKL-KAN1, and DKL-KAN2, as the neural network maps to two output features, allowing for the use of SKI. Conversely, we use KISS-GP with product structure kernel (SKIP) for the standard GP, since the input features are not reduced before being fed to the base kernel.

As illustrated in Table 1, DKL-KAN1 shows superior performance on datasets with a low number of observations. Additionally, we observe that increasing the complexity of the KAN architecture leads to notable improvements in test prediction accuracy. However, for datasets with a large number of observations, DKL-MLP outperforms DKL-KAN, suggesting that the current iteration of KANs is less effective for large datasets. However, we do see DKL-KAN1 outperform all other GP models for `ctslice` dataset.

Table 4 illustrates the RMSE performance of these GP models with an increased number of partitions (i.e., 20) for datasets with a large number of observations. Due to increased partitions (which means using lesser data to train on), we did not consider using SKI/SKI for generating these results. It is evident that for these large datasets, increasing

Table 1: RMSE performance of different GP models on UCI regression datasets with n observations and d input dimensions. The results are averaged over 5 equal partitions (90% train, 10% test) of the data with one standard deviation.

Datasets	n	d	SKI/SKIP used (for scalability)	GP	DKL-MLP	DKL-KAN1	DKL-KAN2
Solar	1066	10	No	1.07 ± 0.32	1.41 ± 0.36	1.04 ± 0.20	1.13 ± 0.31
Airfoil	1503	5	No	2.83 ± 0.85	3.67 ± 0.67	2.21 ± 0.42	2.5 ± 0.55
Wine	1599	11	No	0.55 ± 0.08	0.63 ± 0.15	0.53 ± 0.07	0.54 ± 0.09
Gas	2565	128	No	0.16 ± 0.04	0.15 ± 0.04	0.15 ± 0.03	0.15 ± 0.06
Skillcraft	3338	19	No	0.27 ± 0.04	0.35 ± 0.04	0.27 ± 0.04	0.28 ± 0.04
SML	4137	26	No	0.72 ± 0.08	1.18 ± 0.17	0.69 ± 0.11	0.88 ± 0.19
Parkinsons	5875	20	No	3.85 ± 2.93	11.72 ± 10.78	6.27 ± 2.14	13.26 ± 11.54
Pumadyn	8192	32	No	0.29 ± 0.00	1.2 ± 0.3	0.83 ± 0.26	1.52 ± 0.96
Elevators	16599	18	No	0.14 ± 0.01	0.32 ± 0.27	0.13 ± 0.04	0.15 ± 0.02
Kin40k	40000	8	Yes	0.32 ± 0.03	0.29 ± 0.05	0.30 ± 0.06	0.33 ± 0.08
Protein	45730	9	Yes	0.47 ± 0.01	0.45 ± 0.02	0.46 ± 0.04	0.46 ± 0.03
Tamielelectric	45781	3	Yes	0.29 ± 0.00	0.55 ± 0.09	0.59 ± 0.07	0.59 ± 0.14
KEGG	48827	22	Yes	0.34 ± 0.23	0.30 ± 0.20	0.31 ± 0.21	0.33 ± 0.20
Ctslice	53500	385	Yes	5.14 ± 0.09	3.19 ± 0.12	3.11 ± 0.14	3.21 ± 0.19
KEGGU	63608	27	Yes	0.25 ± 0.17	0.24 ± 0.09	0.25 ± 0.11	0.26 ± 0.10

Table 2: Total number of trainable parameters of different GP models on UCI regression datasets

Datasets	GP	DKL-MLP	DKL-KAN1	DKL-KAN2
Solar	13	536657	5351005	436485
Airfoil	8	531657	5301005	423685
Wine	14	537657	5361005	439045
Gas	131	654657	6531005	738565
Skillcraft	22	545657	5441005	459525
SML	29	552657	5511005	477445
Parkinsons	23	546657	5451005	462085
Pumadyn	35	558657	5571005	492805
Elevators	21	544657	5431005	456965
Kin40k	11	534657	5331005	431365
Protein	12	535657	5341005	433925
Tamielelectric	6	529657	5281005	418565
KEGG	23	546657	5451005	462085
Ctslice	388	911657	9101005	1396485
KEGGU	30	553657	5521005	480005

Table 3: Average computational training runtime (in s) of different GP models on UCI regression datasets (Compute: NVIDIA A100-SXM4-40GB chip (1 GPU with 512 GB RAM))

Datasets	GP	DKL-MLP	DKL-KAN1	DKL-KAN2
Solar	9.83	17.13	33.6	25.19
Airfoil	9	17.09	50.44	31.12
Wine	10.63	17.97	47.6	32.7
Gas	11.98	19.56	86.37	43.07
Skillcraft	11.96	20.99	62.77	34.4
SML	10.12	19.71	61.92	33.4
Parkinsons	56.97	24.44	74.18	41.67
Pumadyn	31.29	43.4	107.53	72.36
Elevators	182.55	56.72	110.39	122.99
Kin40k	190.39	100.98	122.47	140.22
Protein	250.68	220.46	256.91	240.27
Tamielelectric	120.45	156.21	164.89	159.24
KEGG	190.32	187.59	190.83	180.64
Ctslice	206.38	201.54	257.27	203.71
KEGGU	212.44	213.69	258.63	219.08

Table 4: RMSE performance of different GP models on UCI regression datasets with n observations and d input dimensions. The results are averaged over 20 equal partitions (90% train, 10% test) of the data with one standard deviation.

Datasets	n	d	SKI/SKIP used (for scalability)	GP	DKL-MLP	DKL-KAN1	DKL-KAN2
Kin40k	40000	8	No	0.39 ± 0.04	0.42 ± 0.06	0.31 ± 0.10	0.35 ± 0.09
Protein	45730	9	No	0.53 ± 0.03	0.55 ± 0.05	0.51 ± 0.08	0.56 ± 0.09
Tamielectric	45781	3	No	0.29 ± 0.01	0.64 ± 0.11	0.62 ± 0.12	0.63 ± 0.12
KEGG	48827	22	No	0.13 ± 0.02	0.11 ± 0.06	0.10 ± 0.06	0.12 ± 0.07
Ctslice	53500	385	No	6.21 ± 0.16	6.59 ± 0.23	6.19 ± 0.05	6.43 ± 0.06
KEGGU	63608	27	No	0.34 ± 0.15	0.34 ± 0.13	0.31 ± 0.17	0.33 ± 0.15

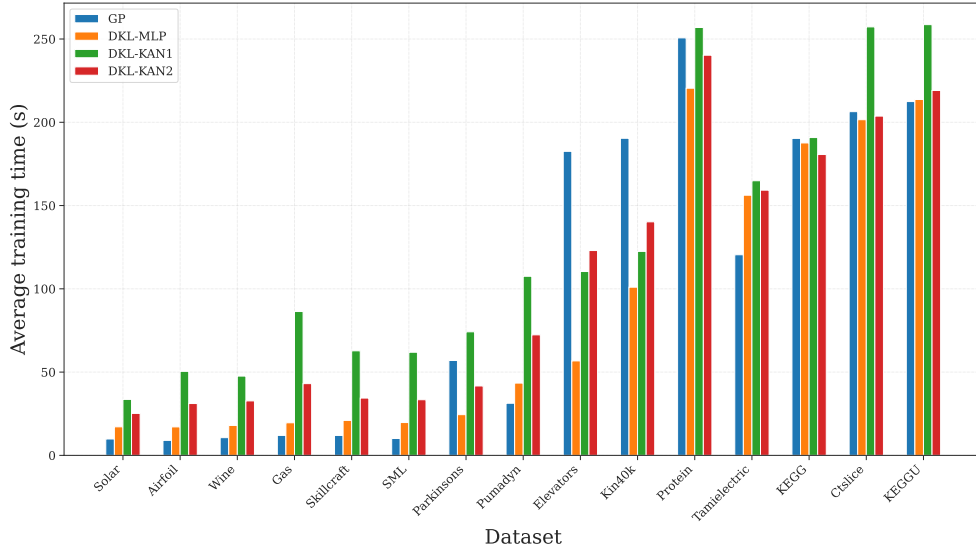


Figure 2: Average training time vs datasets (Compute: NVIDIA A100-SXM4-40GB chip (1 GPU with 512 GB RAM))

the number of partitions leads to better test prediction accuracy of DKL-KAN1 over DKL-MLP, further validating our earlier assertion that KANs in their current version are not scalable to large datasets.

There are also several instances where a standard GP shows relatively better performance than DKL. Table 2 presents the total number of trainable parameters for these models, while Table 3 provides the average computational training time (in seconds) for each model on specific datasets. Given that we used efficient KANs in this study, the training time of DKL-KANs is comparable to that of other GP models (Fig. 2).

5.2.2 Step function

To evaluate the effectiveness of DKL-KAN in handling discontinuities and accurately estimating prediction uncertainty, we consider the step function depicted below

$$y = f(x) + w, \quad w \sim \mathcal{N}(0, 0.01^2),$$

$$f(x) = \begin{cases} 0 & \text{if } x \leq 0 \\ 1 & \text{if } x > 0 \end{cases} \quad (2)$$

For the training process, 100 input points are sampled from a standard normal distribution, whereas the test set consists of 500 datapoints uniformly distributed between -5 and 5 . Given that we are modeling a step function, a neural network with a single hidden layer of 6 neurons is used for both DKL-MLP and DKL-KAN, with the reduced latent dimension set to 2. Fig. 3 illustrates the predictive mean and uncertainty bands when different GP variants are tested on the test set. We observe a relative decrease in epistemic uncertainty in regions where training datapoints are present for GP, DKL-MLP, and DKL-KAN. The standard GP, which assumes a smooth function structure, struggles to model the discontinuity effectively. Due to DKL’s joint supervised learning of input transformation and regression, the neural network captures the discontinuity in the reduced 2D feature space for both MLP and KAN (Fig.4), facilitating a smooth

mapping from reduced feature space to output that the GP can handle (Calandra et al. [2016]). Additionally, we observe that DKL-MLP maintains low uncertainty across the entire function domain as explained in Calandra et al. [2016]. In contrast, DKL-KAN exhibits increasing epistemic uncertainty in regions where training data is not present. The behavior of DKL-MLP with respect to uncertainty bounds is not ideal, as, in an optimal scenario, epistemic uncertainty should rise in areas lacking training data. DKL-KAN, however, offers a balanced solution by accurately capturing discontinuities and appropriately estimating prediction uncertainties.

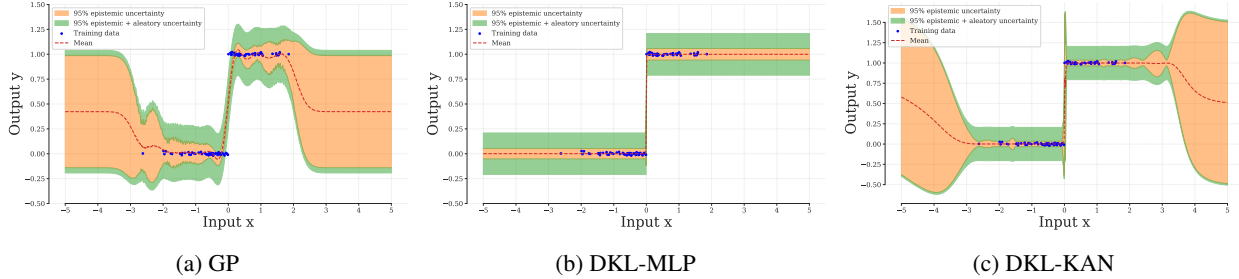


Figure 3: GP prediction

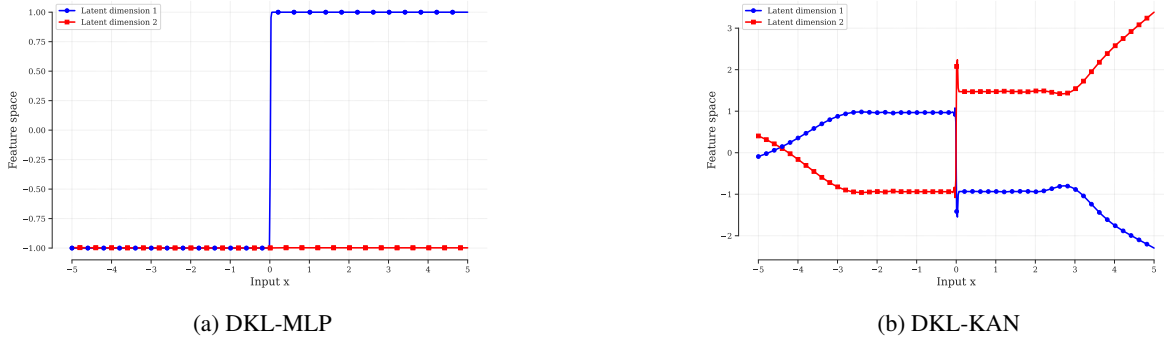


Figure 4: Learned mapping

6 Conclusions

In this study, we investigate the effectiveness of incorporating KANs into DKL. To ensure a fair comparison with DKL-MLP, we train two GP models using KANs: one with an identical number of neurons and layers as the MLP (DKL-KAN1) and another with approximately same number of trainable parameters (DKL-KAN2). Our findings indicate a relatively better performance of KANs when using a larger number of neurons for a fixed number of hidden layers. Moreover, DKL-KANs demonstrate superior performance compared to other GP models on datasets with a low number of observations. Conversely, DKL-MLP exhibit better scalability and higher test prediction accuracy on datasets with a large number of observations. This suggests that, in their current form, KANs are less effective for training on larger datasets. Additionally, DKL-KAN accurately captures discontinuities and prediction uncertainties, particularly in regions lacking training data. The ability of DKL-KAN to increase epistemic uncertainty where data is sparse ensures a more reliable model performance in practical applications.

Acknowledgements

This work is supported by RTX Technology Research Center.

References

Christopher KI Williams and Carl Edward Rasmussen. *Gaussian processes for machine learning*, volume 2. MIT press Cambridge, MA, 2006.

- Tomas Mikolov, Martin Karafiát, Lukas Burget, Jan Cernocký, and Sanjeev Khudanpur. Recurrent neural network based language model. In *Interspeech*, volume 2, pages 1045–1048. Makuhari, 2010.
- Alex Krizhevsky, Ilya Sutskever, and Geoffrey E Hinton. Imagenet classification with deep convolutional neural networks. *Advances in neural information processing systems*, 25, 2012.
- Geoffrey Hinton, Li Deng, Dong Yu, George E Dahl, Abdel-rahman Mohamed, Navdeep Jaitly, Andrew Senior, Vincent Vanhoucke, Patrick Nguyen, Tara N Sainath, et al. Deep neural networks for acoustic modeling in speech recognition: The shared views of four research groups. *IEEE Signal processing magazine*, 29(6):82–97, 2012.
- Andrew Wilson and Ryan Adams. Gaussian process kernels for pattern discovery and extrapolation. In *International conference on machine learning*, pages 1067–1075. PMLR, 2013.
- Yann LeCun, Yoshua Bengio, and Geoffrey Hinton. Deep learning. *nature*, 521(7553):436–444, 2015.
- Chuan Guo, Geoff Pleiss, Yu Sun, and Kilian Q Weinberger. On calibration of modern neural networks. In *International conference on machine learning*, pages 1321–1330. PMLR, 2017.
- Andrew Gordon Wilson, Zhiting Hu, Ruslan Salakhutdinov, and Eric P Xing. Deep kernel learning. In *Artificial intelligence and statistics*, pages 370–378. PMLR, 2016a.
- Simon Haykin. *Neural networks: a comprehensive foundation*. Prentice Hall PTR, 1998.
- Kurt Hornik, Maxwell Stinchcombe, and Halbert White. Multilayer feedforward networks are universal approximators. *Neural networks*, 2(5):359–366, 1989.
- Miles Cranmer. Interpretable machine learning for science with pysr and symbolicregression. jl. *arXiv preprint arXiv:2305.01582*, 2023.
- Ziming Liu, Yixuan Wang, Sachin Vaidya, Fabian Ruehle, James Halverson, Marin Soljačić, Thomas Y Hou, and Max Tegmark. Kan: Kolmogorov-arnold networks. *arXiv preprint arXiv:2404.19756*, 2024.
- Andrei Nikolaevich Kolmogorov. On the representation of continuous functions of many variables by superposition of continuous functions of one variable and addition. In *Doklady Akademii Nauk*, volume 114, pages 953–956. Russian Academy of Sciences, 1957.
- Jürgen Braun and Michael Griebel. On a constructive proof of kolmogorov’s superposition theorem. *Constructive approximation*, 30:653–675, 2009.
- Trefor Evans. Uci datasets. https://github.com/treforevans/uci_datasets, 2021. Accessed: 2024-06-20.
- Andrew Wilson and Hannes Nickisch. Kernel interpolation for scalable structured gaussian processes (kiss-gp). In *International conference on machine learning*, pages 1775–1784. PMLR, 2015.
- Jacob Gardner, Geoff Pleiss, Ruihan Wu, Kilian Weinberger, and Andrew Wilson. Product kernel interpolation for scalable gaussian processes. In *International Conference on Artificial Intelligence and Statistics*, pages 1407–1416. PMLR, 2018.
- Radford M Neal and Radford M Neal. Priors for infinite networks. *Bayesian learning for neural networks*, pages 29–53, 1996.
- Jaehoon Lee, Yasaman Bahri, Roman Novak, Samuel S Schoenholz, Jeffrey Pennington, and Jascha Sohl-Dickstein. Deep neural networks as gaussian processes. *arXiv preprint arXiv:1711.00165*, 2017.
- Alexander G de G Matthews, Mark Rowland, Jiri Hron, Richard E Turner, and Zoubin Ghahramani. Gaussian process behaviour in wide deep neural networks. *arXiv preprint arXiv:1804.11271*, 2018.
- Adrià Garriga-Alonso, Carl Edward Rasmussen, and Laurence Aitchison. Deep convolutional networks as shallow gaussian processes. *arXiv preprint arXiv:1808.05587*, 2018.
- Roman Novak, Lechao Xiao, Jaehoon Lee, Yasaman Bahri, Greg Yang, Jiri Hron, Daniel A Abolafia, Jeffrey Pennington, and Jascha Sohl-Dickstein. Bayesian deep convolutional networks with many channels are gaussian processes. *arXiv preprint arXiv:1810.05148*, 2018.
- Greg Yang. Scaling limits of wide neural networks with weight sharing: Gaussian process behavior, gradient independence, and neural tangent kernel derivation. *arXiv preprint arXiv:1902.04760*, 2019.
- Andrew G Wilson, Zhiting Hu, Russ R Salakhutdinov, and Eric P Xing. Stochastic variational deep kernel learning. *Advances in neural information processing systems*, 29, 2016b.
- Roberto Calandra, Jan Peters, Carl Edward Rasmussen, and Marc Peter Deisenroth. Manifold gaussian processes for regression. In *2016 International joint conference on neural networks (IJCNN)*, pages 3338–3345. IEEE, 2016.
- Maruan Al-Shedivat, Andrew Gordon Wilson, Yunus Saatchi, Zhiting Hu, and Eric P Xing. Learning scalable deep kernels with recurrent structure. *Journal of Machine Learning Research*, 18(82):1–37, 2017.

- Idan Achituve, Aviv Shamsian, Aviv Navon, Gal Chechik, and Ethan Fetaya. Personalized federated learning with gaussian processes. *Advances in Neural Information Processing Systems*, 34:8392–8406, 2021.
- Haitao Liu, Yew-Soon Ong, Xiaomo Jiang, and Xiaofang Wang. Deep latent-variable kernel learning. *IEEE Transactions on Cybernetics*, 52(10):10276–10289, 2021.
- Idan Achituve, Gal Chechik, and Ethan Fetaya. Guided deep kernel learning. In *Uncertainty in Artificial Intelligence*, pages 11–21. PMLR, 2023.
- Sebastian W Ober, Carl E Rasmussen, and Mark van der Wilk. The promises and pitfalls of deep kernel learning. In *Uncertainty in Artificial Intelligence*, pages 1206–1216. PMLR, 2021.
- Alan LS Matias, César Lincoln Mattos, João Paulo Pordeus Gomes, and Diego Mesquita. Amortized variational deep kernel learning. In *Forty-first International Conference on Machine Learning*.
- Jinfeng Xu, Zheyu Chen, Jinze Li, Shuo Yang, Wei Wang, Xiping Hu, and Edith C-H Ngai. Fourierkan-gcf: Fourier kolmogorov-arnold network—an effective and efficient feature transformation for graph collaborative filtering. *arXiv preprint arXiv:2406.01034*, 2024.
- Zavareh Bozorgasl and Hao Chen. Wav-kan: Wavelet kolmogorov-arnold networks. *arXiv preprint arXiv:2405.12832*, 2024.
- Ziyao Li. Kolmogorov-arnold networks are radial basis function networks. *arXiv preprint arXiv:2405.06721*, 2024.
- Alireza Afzal Aghaei. fkan: Fractional kolmogorov-arnold networks with trainable jacobi basis functions. *arXiv preprint arXiv:2406.07456*, 2024a.
- Hoang-Thang Ta. Bsrbf-kan: A combination of b-splines and radial basic functions in kolmogorov-arnold networks. *arXiv preprint arXiv:2406.11173*, 2024.
- Alireza Afzal Aghaei. rkan: Rational kolmogorov-arnold networks. *arXiv preprint arXiv:2406.14495*, 2024b.
- Eric AF Reinhardt and Sergei Gleyzer. Sinekan: Kolmogorov-arnold networks using sinusoidal activation functions. *arXiv preprint arXiv:2407.04149*, 2024.
- Sidharth SS. Chebyshev polynomial-based kolmogorov-arnold networks: An efficient architecture for nonlinear function approximation. *arXiv preprint arXiv:2405.07200*, 2024.
- Khemraj Shukla, Juan Diego Toscano, Zhicheng Wang, Zongren Zou, and George Em Karniadakis. A comprehensive and fair comparison between mlp and kan representations for differential equations and operator networks. *arXiv preprint arXiv:2406.02917*, 2024.
- Yizheng Wang, Jia Sun, Jinshuai Bai, Cosmin Anitescu, Mohammad Sadegh Eshaghi, Xiaoying Zhuang, Timon Rabczuk, and Yinghua Liu. Kolmogorov arnold informed neural network: A physics-informed deep learning framework for solving pdes based on kolmogorov arnold networks. *arXiv preprint arXiv:2406.11045*, 2024.
- Diab W Abueidda, Panos Pantidis, and Mostafa E Mobasher. Deepokan: Deep operator network based on kolmogorov arnold networks for mechanics problems. *arXiv preprint arXiv:2405.19143*, 2024.
- Basim Azam and Naveed Akhtar. Suitability of kans for computer vision: A preliminary investigation. *arXiv preprint arXiv:2406.09087*, 2024.
- Chenxin Li, Xinyu Liu, Wuyang Li, Cheng Wang, Hengyu Liu, and Yixuan Yuan. U-kan makes strong backbone for medical image segmentation and generation. *arXiv preprint arXiv:2406.02918*, 2024.
- Mehrdad Kiamari, Mohammad Kiamari, and Bhaskar Krishnamachari. Gkan: Graph kolmogorov-arnold networks. *arXiv preprint arXiv:2406.06470*, 2024.
- Blealtan. Efficient kan. <https://github.com/Blealtan/efficient-kan>, 2024. Accessed: 2024-06-20.
- Andrew Gordon Wilson, Christoph Dann, and Hannes Nickisch. Thoughts on massively scalable gaussian processes. *arXiv preprint arXiv:1511.01870*, 2015.
- Edward Snelson and Zoubin Ghahramani. Sparse gaussian processes using pseudo-inputs. *Advances in neural information processing systems*, 18, 2005.
- James Hensman, Nicolo Fusi, and Neil D Lawrence. Gaussian processes for big data. *arXiv preprint arXiv:1309.6835*, 2013.
- Bernhard W Silverman. Some aspects of the spline smoothing approach to non-parametric regression curve fitting. *Journal of the Royal Statistical Society: Series B (Methodological)*, 47(1):1–21, 1985.
- Joaquin Quinero-Candela and Carl Edward Rasmussen. A unifying view of sparse approximate gaussian process regression. *The Journal of Machine Learning Research*, 6:1939–1959, 2005.

Andrew Gordon Wilson. *Covariance kernels for fast automatic pattern discovery and extrapolation with Gaussian processes*. PhD thesis, University of Cambridge Cambridge, UK, 2014.

Yunus Saatçi. *Scalable inference for structured Gaussian process models*. PhD thesis, Citeseer, 2012.

John P Cunningham, Krishna V Shenoy, and Maneesh Sahani. Fast gaussian process methods for point process intensity estimation. In *Proceedings of the 25th international conference on Machine learning*, pages 192–199, 2008.